Interaction corrections to two-dimensional hole transport in the large-r_s limit

H. Noh,[1] M. P. Lilly,[2] D. C. Tsui,[1] J. A. Simmons,[2] E. H. Hwang,[3] S. Das Sarma,[3] L. N. Pfeiffer,[4] and K. W. West[4]
[1]*Department of Electrical Engineering, Princeton University, Princeton, New Jersey 08544, USA*
[2]*Sandia National Laboratories, Albuquerque, New Mexico 87185, USA*
[3]*Condensed Matter Theory Center, Department of Physics, University of Maryland, College Park, Maryland 20742, USA*
[4]*Bell Labs, Lucent Technologies, Murray Hill, New Jersey 07974, USA*
(Received 17 December 2002; revised manuscript received 5 May 2003; published 13 October 2003)

The metallic conductivity of dilute two-dimensional holes in a GaAs heterojunction insulated-gate field-effect transistor with extremely high mobility and large r_s is found to have a linear dependence on temperature, consistent with the theory of interaction corrections in the ballistic regime. Phonon scattering contributions are negligible in the temperature range of our interest, allowing comparison between our measured data and theory without any phonon subtraction. The magnitude of the Fermi liquid interaction parameter F_0^σ determined from the experiment, however, decreases with increasing r_s for $r_s \gtrsim 22$, a behavior unexpected from theoretical calculations valid for small r_s.

DOI: 10.1103/PhysRevB.68.165308 PACS number(s): 73.40.−c, 71.30.+h

In two-dimensional (2D) charge carrier systems, it is well known that any amount of disorder in the absence of interactions between the carriers will localize the carriers, leading to an insulator with zero conductivity (σ) as the temperature (T) is decreased to zero.[1] Recent experiments on high-mobility dilute 2D systems, on the other hand, have shown a ''metallic'' behavior at low T, characterized by an increasing σ with decreasing T, and an apparent metal-insulator transition (MIT) as the carrier density is lowered.[2] There are three important energy scales in these systems. The first two are the Fermi energy and interaction energy. Their ratio, which is r_s, is around 10 or higher for the systems where the MIT is observed, implying that an interaction must be playing a role. The other energy scale is related to the disorder in the system given by $\hbar/\tau$, where τ is the elastic scattering time. It has been found from more recent experiments that disorder is also playing a significant role. In particular, the critical density (n_c for electrons and p_c for holes), above which a system shows metallic behavior, is found to decrease when disorder in the 2D system is decreased.[3]

An important question is whether this apparent metallic state is truly a new ground state of the 2D charge carriers or simply a novel finite-temperature behavior of the 2D gas, since all experiments are done at finite T. What is measured in such an experiment is the temperature coefficient $d\sigma/dT$. The metallic behavior evinced by the observation of negative $d\sigma/dT$ at finite T does not necessarily mean, however, a true metal with nonzero conductivity at $T=0$. Recently, Zala *et al.*[4] calculated the Fermi liquid interaction corrections to the conductivity in the asymptotic low-temperature regime ($T/T_F \ll 1$ where T_F is the Fermi temperature) and pointed out that the metallic behavior seen in the high-mobility samples could be understood by taking account of interaction corrections in the ''high-temperature'' ballistic regime ($k_B T > \hbar/\tau$). They found that the conductivity of interacting 2D carriers changes linearly with T in the ballistic regime $T_F \gg T > \hbar/k_B\tau$, with the sign as well as the magnitude of $d\sigma/dT$ depending on the strength of the interaction, while in the low-temperature diffusive regime ($k_B T \ll \hbar/\tau$) the conventional logarithmically changing conductivity[5] is recovered. A linear dependence of σ on T has also been predicted in earlier theories[6,7] based on temperature-dependent screening, and this screening contribution is included in the theory by Zala *et al.*

Experimentally, however, it is not straightforward to identify the interaction corrections unequivocally in the ballistic regime for two main reasons. First, scattering by phonons can give significant contributions at high temperatures. In order to have the ballistic regime at sufficiently low T to minimize the phonon contributions, the 2D charge carrier system must have a very high mobility so that $\hbar/k_B\tau$ becomes very low. Second, the temperature constraint $T_F \gg T > \hbar/k_B\tau$ satisfying the dual conditions of being in the ballistic regime (i.e., $T > \hbar/k_B\tau$, which is a high-temperature constraint) and of also being in the asymptotic low-temperature regime of $T \ll T_F$ (so that the thermal expansion in T/T_F, essential for obtaining the linear-T term in the conductivity, applies) is not easily satisfied experimentally, and indeed most experimentally measured $\rho(T)$ data in 2D systems do not manifest any clear-cut linear-T behavior at low temperatures. An additional issue we are addressing in this work is whether the theory of interaction corrections to the conductivity can describe 2D transport in the large-r_s limit as well. This is particularly germane in view of the fact that the interaction theory is a systematic many-body diagrammatic expansion in the interaction parameter r_s (albeit an infinite-order formal expansion), and the question of the radius of convergence of such an r_s expansion becomes quite important for the large r_s values obtained in our samples.

In this paper, we report our experiments on the low-temperature conductivity and in-plane magnetoresistance (MR) of 2D holes with extremely high mobility and very low density ($r_s \approx 17$–80) to study the interaction corrections. From the temperature dependence of the conductivity, we clearly observed a temperature region where the conductivity shows a linear dependence on T even in this large-r_s limit for a range of densities in the metallic side of the transition. However, the Fermi liquid interaction parameter F_0^σ, determined from a comparison of the data with the theory by Zala

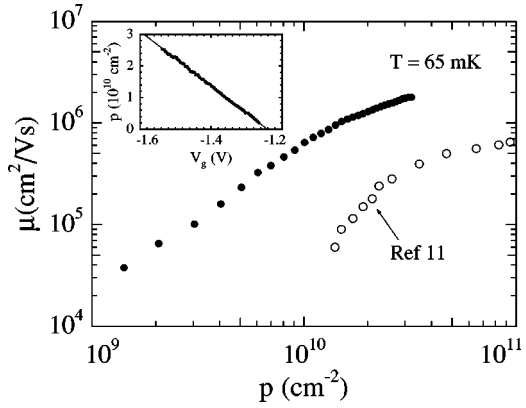

FIG. 1. Mobility vs hole density at $T=65$ mK. Solid circles (●) are from our heterojunction insulated-gate field-effect transistor (HIGFET). Open circles (○) are from conventional modulation doped HEMT structure of Ref. 11 for comparison. Inset shows the hole density vs gate voltage of the HIGFET.

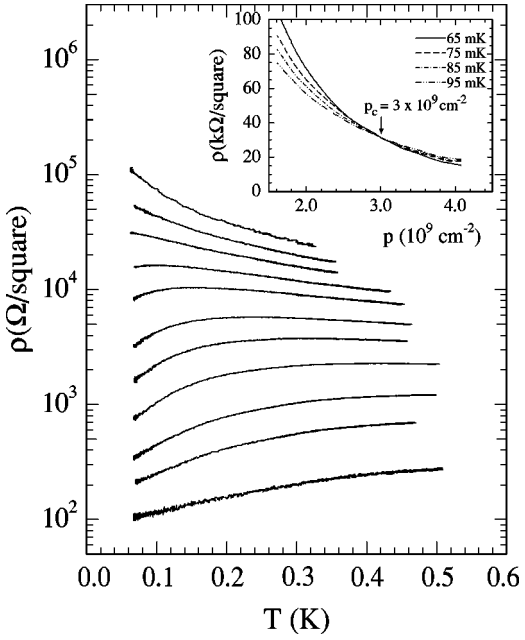

FIG. 2. ρ vs T for $p=3.2$, 2.2, 1.7, 1.2, 0.9, 0.7, 0.5, 0.4, 0.3, 0.23, and 0.15×10^{10} cm^{-2} from the bottom. The inset shows ρ measured as a function of p at different T's. The critical density p_c is marked by an arrow corresponding to a point where ρ is temperature independent.

et al.,[4] shows a surprising nonmonotonic dependence on the carrier density with its value lying between -0.5 and -0.7. F_0^σ increases in magnitude with decreasing density for $p\gtrsim2\times10^{10}$ cm^{-2} ($r_s\lesssim22$) and then decreases with decreasing density for $p\lesssim2\times10^{10}$ cm^{-2} ($r_s\gtrsim22$), a behavior unexpected from a simple extrapolation of the predicted dependence of F_0^σ on small r_s. A separate measurement of effective g factor (g^*) from the in-plane MR provides further confirmation of the unexpected behavior of F_0^σ. g^* decreases with decreasing density, consistent with the behavior expected from F_0^σ for $p\lesssim2\times10^{10}$ cm^{-2} through $g^*=g_b/(1+F_0^\sigma)$.

The sample used in this study is a heterojunction insulated-gate field-effect transistor (HIGFET) made on a (100) surface of GaAs.[8] A metallic gate, separated by an insulator (AlGaAs) from the semiconducting GaAs, is used to induce the 2D holes at the interface between the GaAs and AlGaAs. Ohmic contacts to the 2D holes are made by using a self-aligned contact technique which allows diffusion of the contact material under the gate region. We would like to emphasize that there is no intentional doping in the sample and the 2D holes are induced by the applied gate voltage. This reduces the scattering by ionized impurities so significantly that a very high mobility can be achieved. The mobility (μ) of the sample reaches 1.8×10^6 cm^2/V s at a density (p) of 3.2×10^{10} cm^{-2} (Fig. 1), which is the highest achieved for 2D holes in this low-density regime. This high mobility makes $\hbar/k_B\tau$ for $p=3.2$–0.7×10^{10} cm^{-2} range from 16 mK to 80 mK, low enough that the temperature region where the metallic behavior is observed indeed corresponds to the ballistic regime while phonon contributions are negligible. The extremely high mobility also allows us to measure the temperature dependence of conductivity down to very low densities reaching $p=1.5\times10^9$ cm^{-2}, with r_s near 80.

In Fig. 2, we show the temperature dependence of the resistivity (ρ) at various densities. For $p\geqslant1.7\times10^{10}$ cm^{-2}, ρ decreases monotonically with decreasing T, showing a metallic behavior. For p between 1.2 and 0.4×10^{10} cm^{-2} ρ shows a nonmonotonic dependence on T. It initially increases with decreasing T at high T, which was interpreted as the classical to quantum crossover,[7] and then decreases with decreasing T at low T, showing a metallic behavior as the system goes into the degenerate regime. This crossover shifts to lower temperature with decreasing density and the range where the metallic behavior is seen becomes very narrow, especially for $p=0.5$ and 0.4×10^{10} cm^{-2}. For $p\leqslant3\times10^9$ cm^{-2}, ρ increases monotonically with decreasing T, exhibiting an insulating behavior. To identify the critical density, we measured ρ as a function of p at different temperatures and the data are shown in the inset. The critical density determined from the crossing point, which shows a temperature-independent resistivity, is $p_c=3\times10^9$ cm^{-2}. This low critical density, the lowest ever observed in 2D systems which exhibit the MIT, is consistent with the previous observation by Yoon *et al.*[3] that the critical density becomes lower with decreasing disorder in the system. If we use a hole effective mass $m^*=0.38m_e$, this critical density corresponds to $r_s=57$, which is much larger than the $r_s=37$ predicted for the Wigner crystallization in 2D.[9]

In Fig. 3(a), we replot the data for $p=3.2$–0.7×10^{10} cm^{-2} as σ vs T. The data are scaled by σ_0, the value of σ extrapolated to $T=0$, and T is scaled by $\hbar/\tau k_B$, which is calculated from σ_0 and ranges from 16 mK for $p=3.2\times10^{10}$ cm^{-2} to 80 mK for $p=0.7\times10^{10}$ cm^{-2}. The metallic behavior is identified by increasing σ with decreasing T for all these densities. Clearly, there is a region where σ shows a linear dependence on T as shown by the best fits in the figure with solid lines. We note that r_s for these densities ranges from 17 to 37 and σ shows a linear dependence on T for such large r_s. To compare our results with the theory by Zala *et al.*,[4] we need to consider several points. First, as discussed

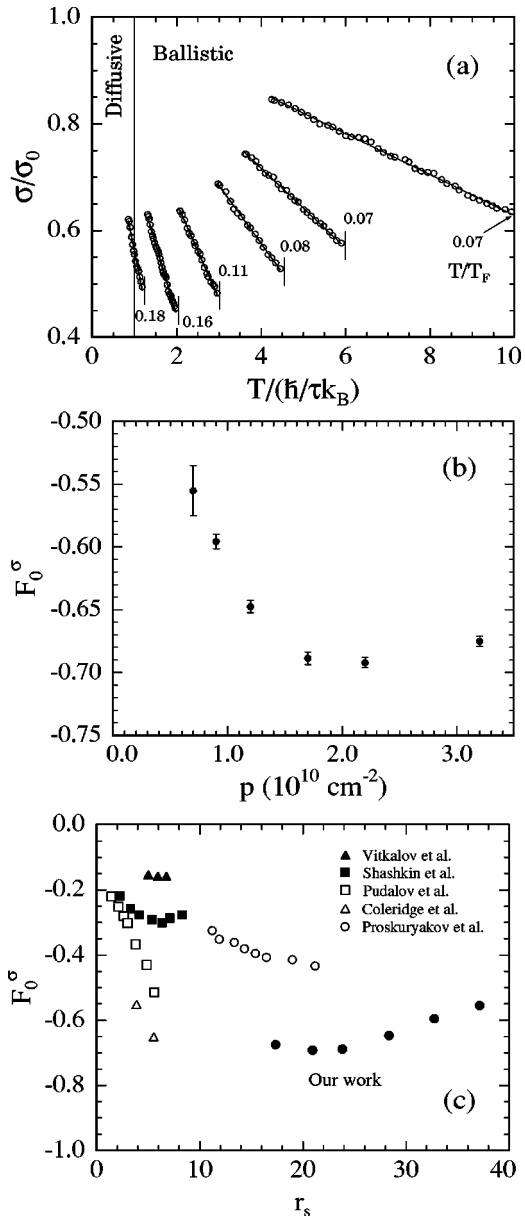

FIG. 3. (a) σ vs T for $p=3.2$, 2.2, 1.7, 1.2, 0.9, and 0.7 $\times 10^{10}$ cm^{-2} from the right to the left. σ is scaled by the value (σ_0) extrapolated to $T=0$, and T is scaled by $\hbar/\tau k_B$. The vertical line at $T/(\hbar/\tau k_B)=1$ is the boundary between the diffusive and the ballistic regime. The solid line for each curve is a linear fit to the data points. Data are truncated above the temperatures indicated in the figure by vertical bars (in units of T_F), where significant deviations from the linear dependence develop. (b) F_0^σ vs p calculated from the slope of the linear dependence in (a). (c) F_0^σ vs r_s, in comparison with results from other experiments indicated.

below phonon contributions are negligible in the temperature range where the linear dependence is observed, which is below 200 mK for $p=3.2\times10^{10}$ cm^{-2} and becomes lower for lower densities. Second, this linear region is indeed in the ballistic regime [$T/(\hbar/\tau k_B)>1$]. Finally, this region is also much lower than the Fermi temperature (T_F) of the system, which is 2.3 K for $p=3.2\times10^{10}$ cm^{-2} and 500 mK for the lowest density $p=0.7\times10^{10}$ cm^{-2}. The data in Fig. 3(a) are below $T=0.07T_F-0.18T_F$. Zala *et al.* have pointed out that the regime where F_0^σ can be treated as a momentum-independent constant is $T\ll(1+F_0^\sigma)^2T_F$. A self-consistency check after we have determined F_0^σ approximately (but somewhat weakly) satisfies this condition. All these allow a direct comparison of our data with their theory. From their theory, the slope of this linear dependence is directly related to the Fermi liquid interaction parameter F_0^σ by the relation

$$\text{slope}=\frac{m^*k_B}{\pi\hbar^2p}\left[1+\frac{3F_0^\sigma}{(1+F_0^\sigma)}\right]. \tag{1}$$

Using $m^*=0.38m_e$,[10] we have obtained from our data F_0^σ as a function of p. The result is shown in Fig. 3(b). The value of F_0^σ lies between -0.5 and -0.7 in the density range we measured from 3.2 to 0.7×10^{10} cm^{-2}. For $p\gtrsim2\times10^{10}$ cm^{-2} ($r_s\lesssim22$), the magnitude of F_0^σ increases with decreasing density. Proskuryakov *et al.*[11] have also found that F_0^σ for 2D holes in (311)*A* GaAs/AlGaAs heterostructure increases in magnitude with decreasing p for $p=2$–8×10^{10} cm^{-2} with values between -0.3 and -0.45. The change of F_0^σ per density is similar in both experiments, while the magnitude of F_0^σ in our measurement is much larger. We note that F_0^σ found from experiments on 2D electrons in Si metal-oxide-semiconductor FET's (MOSFET's) (Ref. 12) also has much smaller magnitude, ranging from -0.14 to -0.5 for electron densities 1–40×10^{11} cm^{-2}, while the value found from *p*-SiGe by Coleridge *et al.*[13] is somewhat comparable to ours, between -0.55 and -0.65. What is surprising in our experiment, which explores the much lower-density (larger-r_s) regime, is that the magnitude of F_0^σ does not increase monotonically with decreasing density. When the density is decreased below 2×10^{10} cm^{-2} ($r_s\gtrsim22$) the magnitude of F_0^σ decreases again (within the error bar). This is opposite to the predicted dependence of F_0^σ on r_s valid for small r_s. To our best knowledge, the dependence of F_0^σ on r_s when r_s is large has not been calculated theoretically, and it is not possible to compare our result with any theoretical predictions at this time.

Experimentally, however, an additional test for this unexpected behavior of F_0^σ can be made from the MR measurements under an in-plane magnetic field ($B_\parallel$). The in-plane MR provides a way to measure the effective g factor, which is directly related to F_0^σ by the relation $g^*/g_b=1/(1+F_0^\sigma)$, where g_b is the bare g factor. Figure 4(a) shows the in-plane MR measured in our sample for various densities at 65 mK. The MR increases as $\exp(B_\parallel^2)$ at low $B_\parallel$ and $\exp(B_\parallel)$ at high $B_\parallel$, consistent with an earlier observation for 2D holes on (311)*A* GaAs.[14] Similarly strong MR has also been observed for 2D electrons in Si-MOSFET's (Ref. 15) and 2D electrons in GaAs.[16] It has been established that this crossover from low-field to high-field dependences corresponds to full spin polarization of the carriers[17] and its position allows the determination of g^*. The crossover field B^*, determined from the position where the second derivative of the ρ vs $B_\parallel$ curve becomes maximum, is marked by an arrow for $p=3.2\times10^{10}$ cm^{-2} in Fig. 4(a), and the dependence of B^* on p is

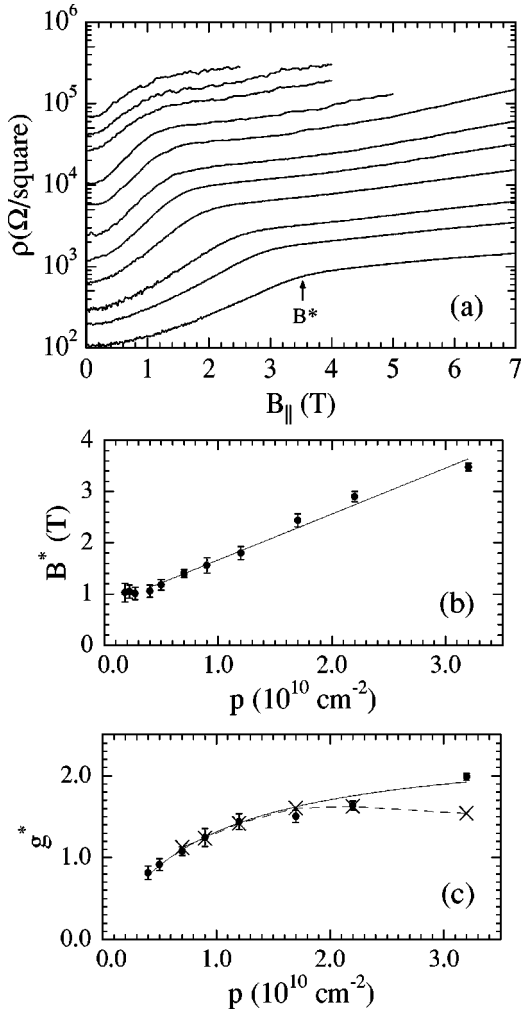

FIG. 4. (a) ρ vs $B_{\parallel}$ at $T=65$ mK and $p=3.2$, 2.2, 1.7, 1.2, 0.9, 0.7, 0.5, 0.4, 0.27, 0.22, and 0.18×10^{10} cm^{-2} from the bottom. B^* is marked by an arrow for $p=3.2\times10^{10}$ cm^{-2}. (b) B^* vs p. The solid line is a linear fit to the data for metallic side, $p>p_c$. (c) Solid circle: g^* determined from B^*. The solid line is the result obtained by the linear fit in (b). Cross: g^* calculated from F_0^σ in Fig. 3(b) using $g^*=g_b/(1+F_0^\sigma)$ and $g_b=0.5$.

shown in Fig. 4(b). For $p>p_c$, B^* decreases linearly with decreasing p (best fit given by the solid line) and saturates in the insulating side of the MIT for $p<p_c$. This behavior is also consistent with earlier observation by Yoon *et al.*[14] for the 2D holes on (311)A. A different way of determining B^*, using the inflection point between high- and low-field dependences, yields a result within the error bar of this plot and produces an error of less than 15% in g^*.

For the metallic side, g^* determined from the relation $2E_F=g^*\mu_B B^*$ (where E_F is the Fermi energy and μ_B is the Bohr magneton) is shown in Fig. 4(c) by solid circles as a function of p. g^* decreases monotonically with decreasing p for the density range measured. The solid line in Fig. 4(c) is the result when the best linear fit in Fig. 4(b) is used. Although an exact quantitative comparison between g^* determined from B^* and that expected from F_0^σ cannot be made since the bare g factor g_b is not well known for holes in

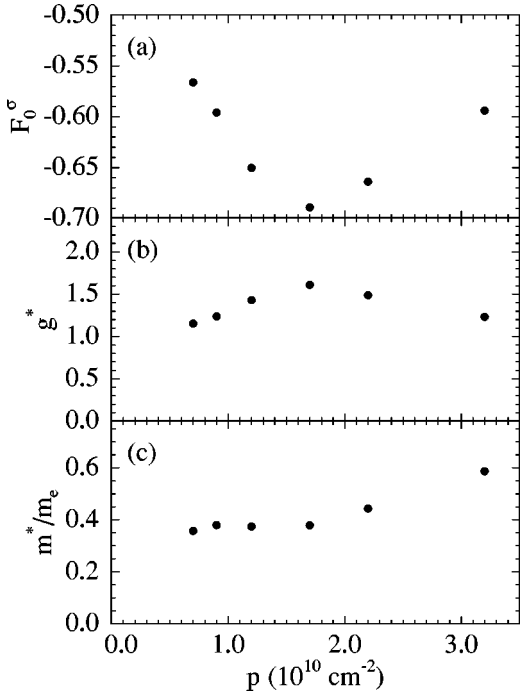

FIG. 5. (a) F_0^σ, (b) g^*, and (c) m^*/m_e vs p calculated from three relations (see the text) without assuming constant m^*.

GaAs, we can vary g_b to find a value which gives the best quantitative agreement. We note that the density dependence of g^* determined from F_0^σ through $g^*=g_b/(1+F_0^\sigma)$ does not depend on a particular value of g_b (g_b itself can depend on density due to spin-orbit effect, but to our best knowledge there is no well-established value of g_b for holes in GaAs). We obtained the best agreement between the two methods with $g_b=0.5$. In Fig. 4(c), g^* determined from F_0^σ is indicated by the crosses. Except for one density $p=3.2\times10^{10}$ cm^{-2}, the values agree surprisingly well. The decrease of g^* with decreasing p is also consistent for $p<2\times10^{10}$ cm^{-2}. While this region of p is where we have observed the unexpected density dependence of F_0^σ, in this region there is good agreement in the behavior of g^*'s determined from two independent methods. Thus, our in-plane MR measurements confirm the unexpected behavior of F_0^σ found from the T dependence of σ.

The decrease in magnitude of F_0^σ with decreasing p (increasing r_s) is of great interest and needs further examination. We therefore have also analyzed our data without the assumption of a density-independent mass $m^*=0.38m_e$. In this analysis, we used three relations among F_0^σ, g^*, and m^* to calculate each quantity. These three relations are Eq. (1), $2E_F=g^*\mu_B B^*$, and $g^*/g_b=1/(1+F_0^\sigma)$. We used $g_b=0.5$, which gave the best quantitative agreement between g^* from the in-plane MR measurements and that from the F_0^σ as seen in Fig. 4(c), although the density dependence of F_0^σ does not depend on a specific value of g_b. The results of the analysis are shown in Fig. 5. m^* found from this analysis is around $0.4m_e$ for $p\leqslant1.7\times10^{10}$ cm^{-2} and increases to $0.6m_e$ for $p=3.2\times10^{10}$ cm^{-2}. F_0^σ again exhibits a nonmonotonic de-

pendence on p. The magnitude of F_0^σ increases with decreasing p for $p \gtrsim 1.5\times10^{10}$ cm^{-2} and decreases with decreasing p for $p \lesssim 1.5\times10^{10}$ cm^{-2}. The decrease of F_0^σ in magnitude with decreasing p for large r_s is still observed and confirmed once again.

Any explanation for this surprising result should take into account the large r_s values in our system. For $r_s \geqslant 37$, the 2D system is expected to be a pinned Wigner crystal. The critical density for MIT in our system corresponds to $r_s = 57$, considerably larger than the critical r_s predicted for this crystallization. The r_s values for which we observed the unexpected behavior of F_0^σ range between 22 and 37, close to that predicted for Wigner crystallization. We note that there has been a Monte Carlo calculation[18] of Fermi liquid parameters for r_s up to 5, where F_0^σ still increases monotonically in magnitude with increasing r_s. To our knowledge, there is no theoretical calculation of the dependence of F_0^σ on r_s when r_s is larger, relevant to our experiment. The question whether the crystallization is preceded by a ferromagnetic instability with $F_0^\sigma = -1$ has to be addressed as well. From Monte Carlo calculations, Tanatar and Ceperley[9] have showed both possibilities of a diverging and a finite-valued spin susceptibility as r_s increases toward the critical r_s for the Wigner crystallization. Our result appears to imply that the ferromagnetic instability does not occur in the large-r_s regime of our 2D hole system.

We now address the important issue of the phonon scattering contribution to our measured hole resistivity, which we have ignored in our analysis. The question of the phonon contribution to the resistivity is crucial since, if it is significant, it would then be impossible to compare our measured resistivity to the interaction theory. We have therefore theoretically directly calculated the screened acoustic phonon scattering contribution to the resistivity by including both the deformation potential and piezoelectric coupling of the 2D holes to 3D acoustic phonons of GaAs. Following Ref. 19 we have carried out a detailed calculation of the phonon scattering contribution to the hole resistivity in the parameter range of our experiment. In this calculation we used $m^* = 0.38 m_e$ and the parameters corresponding to GaAs: $c_l = 5.14\times10^5$ cm/s, $c_t = 3.04\times10^5$ cm/s, $\rho = 5.3$ g/cm^3, $eh_{14} = 1.2\times10^7$ eV/cm, and $D = -8.0$ eV. Our theoretical phonon-only resistivity, as shown in Fig. 6, demonstrates that for $T \leqslant 200$ mK—the temperature regime we concentrate on in comparing our experimental resistivity with the interaction theory—the phonon contribution to the resistivity is miniscule (less than 1% of the measured resistivity). We are therefore justified in neglecting phonon scattering effects in the discussion of our experimental results as long as we restrict ourselves to $T < 200$ mK as we have done in analyzing our data. As is obvious from our theoretical results presented in Fig. 6, the hole-phonon scattering contribution to the hole resistivity becomes non-negligible for $T > 200$ mK and is, in fact, significant for $T \geqslant 500$ mK with its quantitative importance increasing with decreasing carrier density.

We should point out in this context that we disagree with the methodology employed recently by Proskuryakov *et al.*[11] in subtracting out a calculated phonon scattering contribution to their measured resistivity in analyzing their hole transport data in the context of a quantitative comparison with the interaction theory of Zala *et al.*[4] First, it is well known[20] that Matthiessen's rule does not apply to 2D systems at finite temperatures, and therefore, subtraction of the phonon contribution (even if this contribution were accurately known, which is questionable) in order to obtain the nonphonon part is unjustified and may be subject to large errors. (This problem is worse in the presence of screening of a hole-phonon interaction, which must be included in the theory.) Second, the calculation of the phonon scattering contribution to the hole resistivity, following Ref. 21, carried out by Proskuryakov *et al.*[11] is rather crude and approximate (compared, for example, with our theoretical calculations shown in Fig. 6 of this paper). We note that in Ref. 11 the measured hole resistivity (before any phonon subtraction) hardly manifests any clear-cut linear temperature regime, and the subtracted phonon contribution is a large fraction of the measured resistivity, thereby casting substantial doubt on the accuracy of the subtracted resistivity eventually compared with the interaction theory. Our analysis in this work avoids these serious pitfalls of Ref. 11 by directly considering the measured resistivity in the context of interaction theory, which we justify by explicitly calculating the phonon contribution to the hole resistivity in the temperature range of our interest and showing it to be negligible so that no arbitrary and unjustifiable phonon subtraction is required (in contrast to Ref. 11).

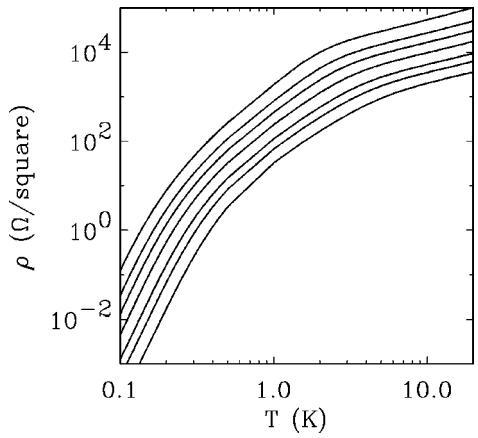

FIG. 6. Resistivity due to phonon scatterings (piezoelectric and deformation potential coupling) as a function of temperature. Here the lines corresponds to the hole density $p = 0.5$, 0.7, 0.9, 1.2, 1.7, 2.2, 3.2×10^{10} cm^{-2} (from top to bottom).

In summary, we have measured the temperature dependence of the metallic conductivity of extremely high-mobility dilute 2D holes in GaAs in the large-r_s limit. We find that the conductivity shows a linear dependence on temperature in the ballistic regime. The Fermi liquid interaction parameter F_0^σ obtained from our data is found to exhibit a nonmonotonic dependence on density and decrease in magnitude with increasing r_s for $r_s \gtrsim 22$.

This work is supported by the NSF and MRSEC at Princeton University and by the U.S. ONR at Maryland.

[1] E. Abrahams, P.W. Anderson, D.C. Licciardello, and T.V. Ramakrishnan, Phys. Rev. Lett. **42**, 673 (1979).
[2] For a review, see B.L. Altshuler, D.L. Maslov, and V.M. Pudalov, Physica E (Amsterdam) **9**, 209 (2001); E. Abrahams, S.V. Kravchenko, and M.P. Sarachik, Rev. Mod. Phys. **73**, 251 (2001).
[3] J. Yoon, C.C. Li, D. Shahar, D.C. Tsui, and M. Shayegan, Phys. Rev. Lett. **82**, 1744 (1999).
[4] G. Zala, B.N. Narozhny, and I.L. Aleiner, Phys. Rev. B **64**, 214204 (2001).
[5] B.L. Altshuler, A.G. Aronov, and P.A. Lee, Phys. Rev. Lett. **44**, 1288 (1980); H. Fukuyama, J. Phys. Soc. Jpn. **48**, 2169 (1980); A.M. Finkelstein, Sov. Phys. JETP **57**, 97 (1983) [Zh. Éksp. Teor. Fiz. **84**, 168 (1983)].
[6] A. Gold and V.T. Dolgopolov, Phys. Rev. B **33**, 1076 (1986); S. Das Sarma, *ibid.* **33**, 5401 (1986).
[7] S. Das Sarma and E.H. Hwang, Phys. Rev. Lett. **83**, 164 (1999); Phys. Rev. B **61**, R7838 (2000).
[8] B.E. Kane *et al.*, Appl. Phys. Lett. **63**, 2132 (1993).
[9] B. Tanatar and D.M. Ceperley, Phys. Rev. B **39**, 5005 (1989).
[10] m^* measured for high-density 2D holes on a (100) surface by cyclotron resonance, H.L. Stormer *et al.*, Phys. Rev. Lett. **51**, 126 (1983); cyclotron resonance experiment for low-density (comparable to our sample) 2D holes on (311)*A* heterostructure also produces similar numbers, S. Bayrakci *et al.* (unpublished).
[11] Y.Y. Proskuryakov, A.K. Savchenko, S.S. Safonov, M. Pepper, M.Y. Simmons, and D.A. Ritchie, Phys. Rev. Lett. **89**, 076406 (2002).
[12] A.A. Shashkin, S.V. Kravchenko, V.T. Dolgopolov, and T.M. Klapwijk, Phys. Rev. B **66**, 073303 (2002); S.A. Vitkalov, K. James, B.N. Narozhny, M.P. Sarachik, and T.M. Klapwijk, *ibid.* **67**, 113310 (2003); V.M. Pudalov, M.E. Gershenson, H. Kojima, G. Brunthaler, A. Prinz, and G. Bauer, cond-mat/0205449 (unpublished).
[13] P.T. Coleridge, A.S. Sachrajda, and P. Zawadzki, Phys. Rev. B **65**, 125328 (2002).
[14] J. Yoon, C.C. Li, D. Shahar, D.C. Tsui, and M. Shayegan, Phys. Rev. Lett. **84**, 4421 (2000).
[15] D. Simonian, S.V. Kravchenko, M.P. Sarachik, and V.M. Pudalov, Phys. Rev. Lett. **79**, 2304 (1997).
[16] E. Tutuc, S. Melinte, and M. Shayegan, Phys. Rev. Lett. **88**, 036805 (2002).
[17] T. Okamoto *et al.*, Phys. Rev. Lett. **82**, 3875 (1999); S.A. Vitkalov *et al.*, *ibid.* **85**, 2164 (2000); V.T. Dolgopolov and A. Gold, JETP Lett. **71**, 27 (2000); I.F. Herbut, Phys. Rev. B **63**, 113102 (2001); E. Tutuc *et al.*, Phys. Rev. Lett. **86**, 2858 (2001).
[18] Y. Kwon, D.M. Ceperley, and R.M. Martin, Phys. Rev. B **50**, 1684 (1994).
[19] T. Kawamura and S. Das Sarma, Phys. Rev. B **42**, 3725 (1990); **45**, 3612 (1992).
[20] F. Stern, Phys. Rev. Lett. **44**, 1469 (1980).
[21] V. Karpus, Semicond. Sci. Technol. **5**, 691 (1990).